

SIMULATING PRESSURE AND VELOCITY TIME SERIES WITH ARTIFICIAL NEURAL NETWORKS: SOME ADVANTAGES AND PITFALLS

Gregory A. Kopp^{*}, Joan Ferre-Gine[†] and Francesc Giralt[#]

^{*} Boundary Layer Wind Tunnel Laboratory, University of Western Ontario
London, ON, N6A 5B9, Canada. TE: 1-(519)-661-3338
e-mail: gak@blwtl.uwo.ca, web page: <http://www.blwtl.uwo.ca/>

[†] Departament d'Enginyeria Informàtica i Matemàtiques, Universitat Rovira i Virgili
Av. Paisos Catalans, 26, Tarragona, 43007, Catalunya, Spain
TE: 34-977-559-687, e-mail: jferrer@etse.urv.es, web page: <http://www.etseq.urv.es/>

[#] Departament d'Enginyeria Química, Universitat Rovira i Virgili
Av. Paisos Catalans, 26, Tarragona, 43007, Catalunya, Spain
TE: 34-977-559-638, e-mail: fgiralt@etseq.urv.es
web page: <http://www.etseq.urv.es/personal/fgiralt/fgiralt.html>

Key words: Artificial Neural Networks, Turbulence, Wakes, Time Series, Simulation.

Abstract. *Three examples of time series simulations of pressure and velocity fluctuations using artificial neural networks were discussed: (i) a spatial interpolation of pressure time series on the roof of a low building in a thick, turbulent boundary layer, (ii) a simulation of two velocity components at multiple spatial locations simultaneously in the turbulent far wake of a circular cylinder, and (iii) a simulation of pressure time series around the surface of a circular cylinder in a crossflow. For the spatial interpolation a backpropagation network was used, while for the other two simulations, the fuzzy ARTMAP neural classifier was used. It was shown that the fuzzy ARTMAP captured the energy of the fluctuations over a wider range of scales than the backpropagation network because of its architecture, even though the input and output types were similar. The fuzzy ARTMAP is based on a clustering-type of pattern recognition while the backpropagation network is more deterministic, i.e., more like an empirical curve-fit to the data. This appears to allow the fuzzy ARTMAP to capture the dynamics of the flow field to a greater extent.*

1 INTRODUCTION

The simulation of the spatial and temporal variations of physical variables in transient processes is important in many engineering applications. Examples include the active control of processes, prediction of system behaviour for the design of a process or product, and forecasting future behaviour based on the current or previous state of a system or process. Often, this is done by solving the equations representing the physical laws that govern the process or system. Other times this is done by solving engineering design equations or empirical models of the system. In fluid mechanics, the governing equations are difficult to solve directly in practical engineering situations because of the “problem” of turbulence. So, approximate forms of the equations are used with empirically based, or calibrated, turbulence models. These often work reasonably well for engineering design purposes, and experimental data are used to confirm the results (or at least calibrate and validate the turbulence models).

Since experiments are often difficult and costly, it makes some sense to consider alternative approaches which make greater use of the data, perhaps with a loss of generality, but with the benefit of increased simplicity or speed. Artificial neural networks offer such approach and are the focus of the current paper, but there are many other methodologies currently under development¹⁻⁴. We will focus on some applications in fluid mechanics and wind engineering which have interested us, mainly on time series simulations of multiple spatially varying variables.

Artificial neural networks (ANN) have many inputs and outputs with nonlinear transfer function in the “neurons”, the connections between the inputs and outputs. Because of these features, they are used for solving multivariate and nonlinear problems. The main drawbacks are that they are costlier (in terms of computational complexity and time consumption) and may not be sufficiently generalized due to limitations in the input or output data, or the choice of these. There is no theoretical basis for determining the optimum neural network configuration. This has to be done on an ad-hoc basis and, therefore, requires an “expert” user. One of the objectives of this paper is to illustrate some of the advantages of using neural networks, one of those being that they can “learn” some of the underlying dynamic behavior and, therefore, make more accurate predictions under a wider variety of circumstances compared to other methods. An example is also shown where the approach did not work accurately because the input was not entirely appropriate to the situation.

2 ARTIFICIAL NEURAL NETWORKS

There is a variety of neural network models⁵⁻⁷. They differ in terms of structure and mode of operation and include multilayer networks, single layer perceptrons, Carpenter networks, Hamming networks and Hopfield networks. Many utilize fuzzy logic to simplify the calculations and inputs, such as the Fuzzy ARTMAP neural network⁸⁻¹², described in more detail below. Probably the most widely used networks are multilayer networks with backpropagation learning using the gradient method. The topology of one such network is shown in Figure 1 for a single hidden layer.

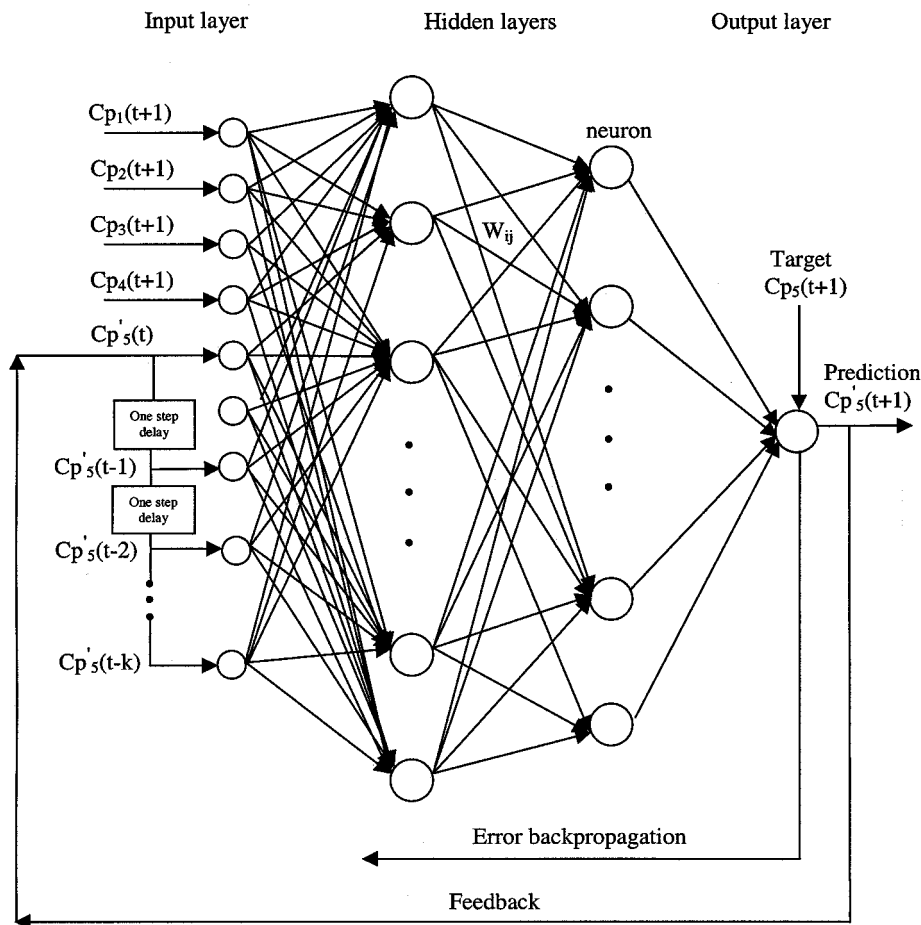


Figure 1: The time-delay back propagation neural network (from [21])

2.1 Backpropagation Networks

Backpropagation neural networks generally have a layered structure with an *input layer*, an *output layer* and one or more “*hidden*” layers between the input and output layers. Each layer is composed of artificial neurons (processing elements), which are represented with circles in Figure 1. Each neuron is connected to all neurons in the layers immediately above and below, via adaptive weights. The neurons in the first layer (*input layer*) only serve in the role of external stimuli, i.e., they transfer the external inputs into the neural system. The *output layer* is the final output of the ANN. Each neuron in hidden layers and output layers receive the weighted input from the output of other neurons from lower layers. The *weights*, measures of the strength of the connections between neurons⁵, are determined via the training process. Neurons in hidden layers and output layers play the most important role in ANN function because they perform the only computations (via their nonlinear transfer function). Each

neuron (except in the input layer) receives a set of weighted inputs from the neurons in the layer below and then produce a corresponding response which is fed-forward to the next layer. By adjusting the weights (connections), an ANN can be trained with the available experimental data set to generalize the functional relationship and produce the desired output for a given set of inputs. There are many training algorithms, but the most frequently used algorithm (to determine the weights) is known as Widrow-Hoff learning or backpropagation algorithm^{5,7,13}.

It is worth noting that one can write the equation for this type of network, although it is extremely tedious. In some sense, determining the weights is not unlike determining constants in a regression analysis, with this type of ANN model really being an elaborate curve fit. In this context, the ANN would be considered “over-parametrized” or overtrained.

2.2 Fuzzy ARTMAP

The Fuzzy ART architecture was designed by Carpenter et al.⁸⁻¹² for multidimensional data clustering based on a set of features. The Fuzzy ARTMAP neural network is formed by a pair of fuzzy ART modules, Art_a and Art_b, linked by an associative memory and an internal controller. To extract structures from the turbulent wake Ferre-Gine et al.^{14,15} proposed a modified version of Fuzzy ARTMAP which was specially conceived to this purpose. The classification procedure of fuzzy ART is based on Fuzzy Set Theory¹⁶. The similarity between two vectors can be established by the grade of the membership function, which for two generic vectors (l, m) can be easily calculated as

$$\text{grade}(\xi^l \subset \xi^m) = \frac{|\xi^l \wedge \xi^m|}{|\xi^l|} \quad (1)$$

where the “ \wedge ” is the fuzzy AND operator and the norm, $|\bullet|$, is the sum of the components of the vector. The mechanisms to speed up the process and to conduct the classification properly can be found elsewhere¹², as can the details for the current applications^{14,15,17}.

Modifications to allow the simulation of time series were made by Giralt et al.¹⁷. Figure 2 depicts a schematic of the network. It is worth emphasizing that the structure of this network is completely different than backpropagation networks, since it does not have a layered structure. Whereas backpropagation behaves more like nonlinear curve fits, the fuzzy ARTMAP relies on data clustering. The problem of determining cluster boundaries is illustrated in Figure 3, which shows two “natural” clusters in a two-dimensional space, easily identifiable by eye. Clustering is the process of separating the data points automatically into classes. Originally, clustering was based on the idea that one particular pattern either belonged or did not belong to a given cluster. Membership of a particular element in the given cluster was either 0 (does not belong) or 1 (does belong). This is called “hard” clustering. Fuzzy logic¹⁶ is a more effective approach to separate clusters. The main difference between fuzzy clustering and hard clustering is that each element has real membership in each cluster, such that the sum of its membership in all clusters is unity.

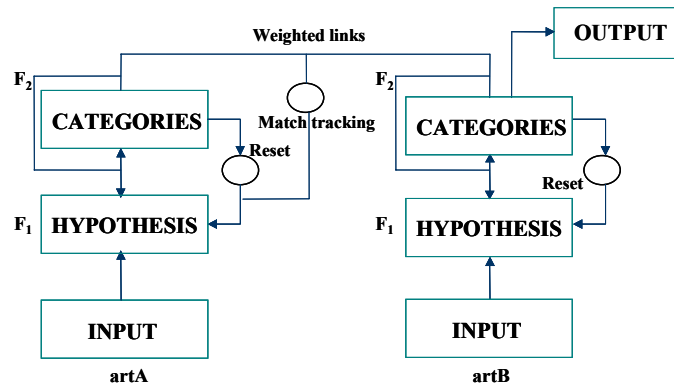


Figure 2: Sketch of the predictive Fuzzy ARTMAP Neural Network (from [17])

For time series simulations, one network of this type was created for each sensor. All the networks operated synchronously and in parallel. Each individual network was first trained with the output in Figure 2 disconnected. The training data for each individual network in the velocity simulation consisted of vectors with 12 elements for the Art_a module, four temporal (or historical) velocity components (u and w) for the probe under consideration, plus the two components from each of the two spatially adjacent probes. The subsequent values of each velocity component in the time sequence (i.e., vectors with two elements) were used for the Art_b module. Thus, simultaneous space-time information was provided to the neural system in terms of the input to each Art_a module, with the corresponding future information for (u , w) given to each Art_b module. There was no other association between individual networks.

The dimension of the input vectors to the eight neural networks and the type of simultaneous space-time information that they contained was decided after examination of the space-time correlation of the experimental data, so that relevant structural (scale) characteristics of the flow were provided to the system during training. The choice of four temporal data for each velocity component in the training input vector is consistent with Takens theorem³⁰. This theorem states that good accuracy can be achieved in point-to-point forecasting in a system with attractors of dimension d when a function that depends at most on $(2d+1)$ past measurements is used. For the data herein, this implies using between four and five historical data in the training sets. Details can be found elsewhere¹⁷.

3 INTERPOLATION TO INCREASE DATA RESOLUTION

One example of the need for time series simulation is to increase the resolution of experimental data when the data is being used for further numerical analyses. Because of both increased computational and experimental capacities, numerical structural analyses of buildings are being performed with the input loading taken directly from experimental data. Currently, we have the capability to measure surface pressures at about 1000 locations simultaneously on the surface of a model building, greater numbers being a matter of only cost (equipment and the costs of running such experiments). Even though this is a large number, numerical (e.g., finite element) analyses of structural responses often require greater

resolution. Thus, interpolation techniques are required. Several approaches could be applied such as linear interpolation, cubic splines (e.g., as Antonia et al.¹⁸ did to increase the resolution of their hot-wire experiments), linear stochastic estimation^{19,20}, etc. We have used a backpropagation ANN for this type of application²¹ as it has several advantages that will be discussed below. Figure 1 illustrates the structure of the network used here.

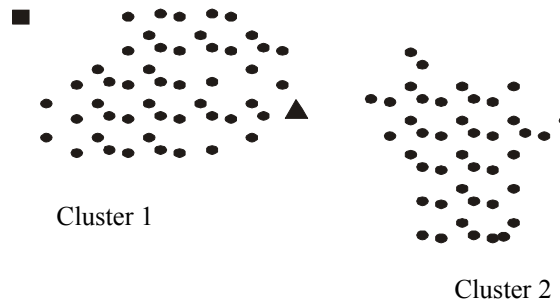


Figure 3: An example of natural clusters in a two-dimensional pattern space (from [28])

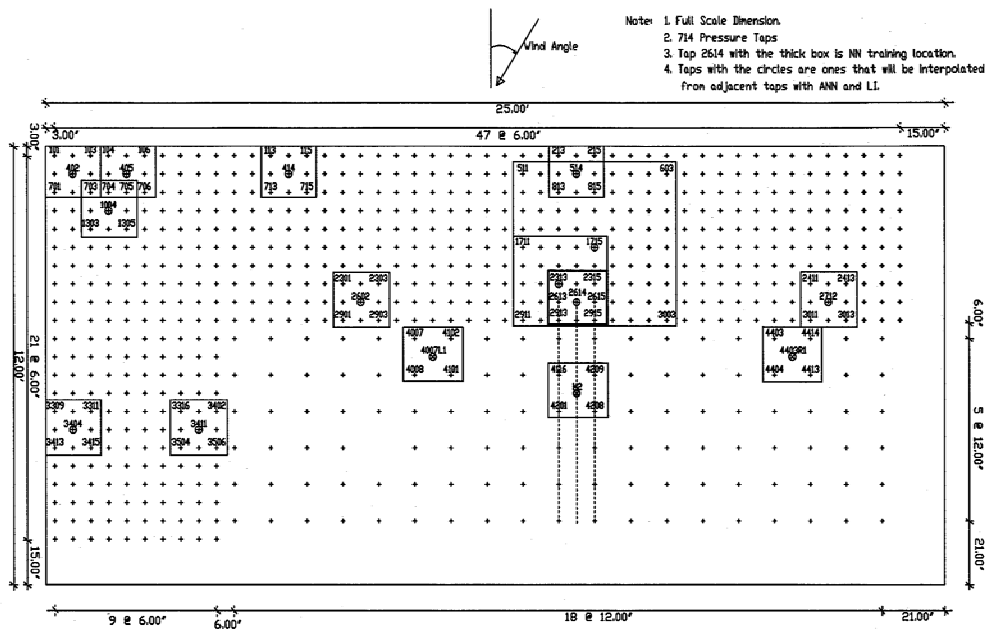


Figure 4: Tap layout and numbering scheme on the roof panel (from [21])

Surface pressures on low buildings depend on many factors including the location on the surface, the building geometry and the characteristics of the upstream boundary layer. For interpolation, most of this information is assumed to be implicitly contained in the pressure data measured at taps adjacent to the location for which we want new data. Thus, these are the only inputs used, as implied by Figure 1, where Cp_5 is the pressure coefficient of the tap we wish to obtain time series for, while Cp_1 , Cp_2 , Cp_3 , Cp_4 are the pressure coefficients from the adjacent taps. Thus, the input is the adjacent pressure coefficients at time, $t+1$, plus the earlier

(i.e., previously forecasted) coefficients of Cp_5 at t , $t-1$, ..., $t-k$. The output is Cp_5 at time, $t+1$. The implication is that the data at the adjacent spatial locations are correlated and that this is really the only relevant parameter in the analysis. This is consistent with the goal of interpolation, but limits the generality of the results. Scales smaller than the spatial distances between taps may be lost, although one would hope that these get picked up to some extent without considering them explicitly. Note that this is somewhat different than for linear interpolation where the assumption is that the new data (Cp_5) is simply an average of the data from the adjacent points, and no small-scale features (“small” meaning smaller than the distance between adjacent taps) are relevant. The use of splines implies a similar assumption. However, the assumptions implicit to this ANN are similar to that of linear stochastic estimation where the covariance matrix is used explicitly^{19,20} so one may expect similar results.

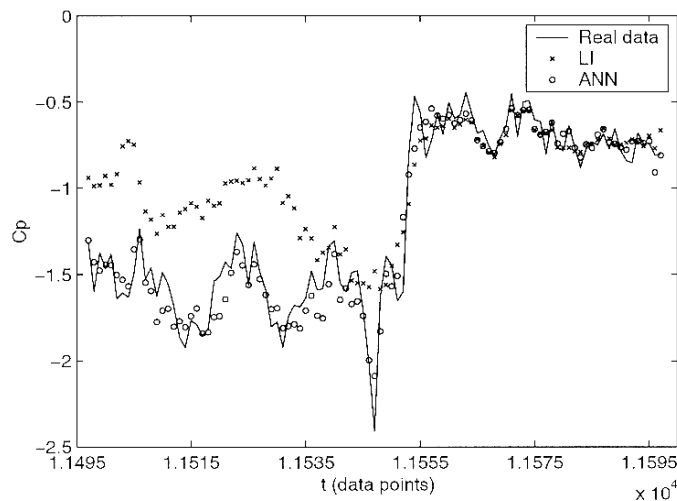


Figure 5 Time series for tap on high resolution panel (from [21])

Pressure time series at more than 700 locations were obtained over a small region of the roof of a low building of large plan dimension in a boundary layer simulating open country terrain. The nominal model scale was 1:50 and Figure 4 shows the equivalent full-scale dimensions. Figure 4 also shows a sketch of the tap locations, some of which will be discussed herein. Further details can be found in Chen, Kopp and Surry²¹. The data have been used by Ali and Senseny²² to perform a finite element analysis of the structural response of the connections between the roof cover and the structural frames (purlins). Figure 5 shows a segment of the actual time series at location #1715 (see Figure 4) along with the interpolated ANN signal and that from linear interpolation where the four adjacent taps are numbered 511, 603, 2911, and 3003 on Figure 4. One can see that the ANN-signal “tracks” the real signal much more closely than that obtained by linear interpolation. The ANN-generated signal captures a reasonably range of the frequency content but starts falling off around 20 Hz, as does the autospectra from the linear interpolation, as shown in Figure 6. The spectra of the error from the ANN-generated signal is like that of white noise, probably due to smaller scale

eddies that do not influence the adjacent taps and the lack of perfect correlation between the interpolated location and the adjacent taps.

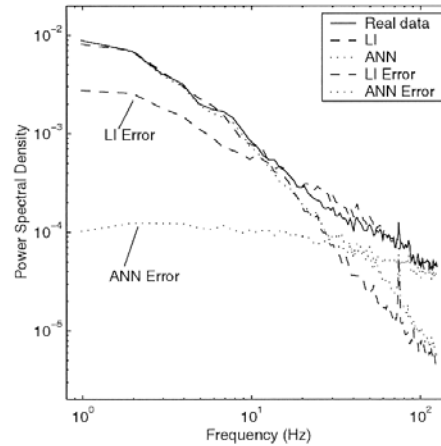


Figure 6: Autospectra of pressure time series for Tap 1715 (from [#])

Some evidence that the ANN has learned the correlation between the adjacent taps can be obtained by considering the output of the same trained net at other spatial locations. In regions where the flow field is broadly similar, the accuracy of the interpolated time series is excellent. However, in the corner of the roof there are large spatial gradients, not only of the magnitudes of the pressure coefficients, but also higher order statistics such as the skewness and kurtosis. The resulting performance of the ANN drops off rapidly. Even a net re-trained with the data from the corner (for tap #402) could not accurately interpolate data in this region. The time series from adjacent taps have low correlations relative to the corner tap, implying that different input from that in Figure 1 is required in order to correctly capture the physics and interpolate the time series.

4 SIMULATION OF TURBULENT VELOCITY FLUCTUATIONS

The dynamics of turbulence involves the interaction of “eddies” of different scales, which results in a transfer of energy from the mean flow primarily to the large scales (or large eddies). Energy is then transferred to correspondingly smaller eddies by the larger ones until it is ultimately dissipated at the smallest (Kolmogorov) scales²³. In fully developed, plane, turbulent wakes, the large eddies are random variables, but have a particular, repeated shape. The available experimental evidence indicates that they are the controlling factor for the spread rate of the turbulence and the overall rates of entrainment or mixing²⁴⁻²⁶. In order to determine these characteristics, we have taken the approach of developing and applying pattern recognition techniques^{14,15,27,28}. The task is reasonably complex because turbulent velocity signals have energy at scales varying by several orders of magnitude. Figure 7 shows time series from segments of 16 sensors (hot-wires) in the wake of circular cylinder, 420 diameters downstream of the cylinder. The basic experimental set-up showing the sensors are shown in Figure 8. Figure 9 shows the autospectra for the velocity data measured at two of

the sensors.

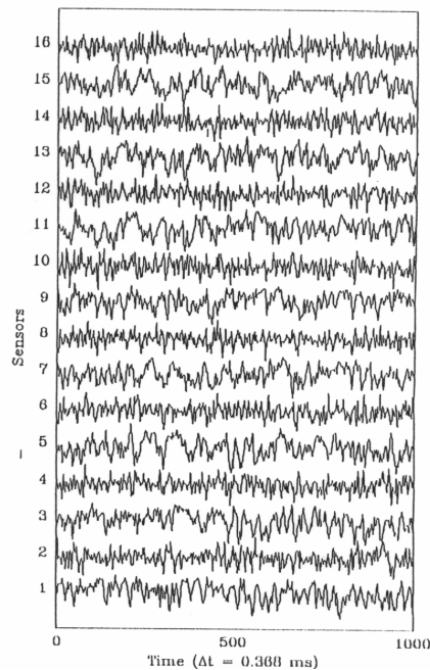


Figure 7: Time series from 16 sensors in a turbulent wake (from [17])

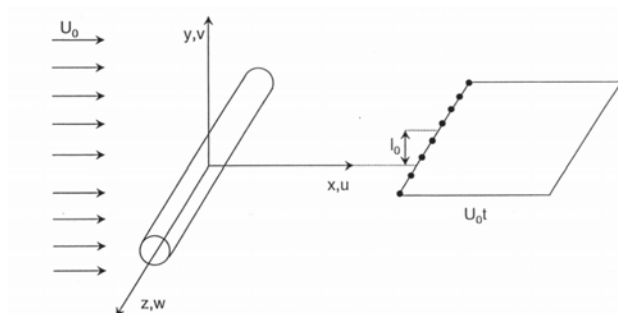


Figure 8: Sketch of the experimental set-up with the sensor (X-wire) locations

Embedded within these seemingly random signals are the large scale eddies which play a key role in the dynamics of the turbulence. Our goal was to simulate these time series by using our knowledge of this, but without using the governing (Navier-Stokes) equations. Giralt and co-workers^{14,15} applied Fuzzy ARTMAP to identify and classify the patterns in these data and modified the network architecture to simulate time series. The idea was simple: since the Fuzzy ARTMAP had already classified the patterns, it should be able to reconstruct a pattern from partial velocity information of the pattern given what it had “learned” in the classification stage. So, if the re-configured net, shown in Figure 2, was given an initial condition it generated velocity data at the next moment in time, and with that, the next, and so on. The results were reported in Giralt et al.¹⁷, where further details can be found, and are briefly summarized here. Essentially, the modified fuzzy ARTMAP neural classifier learned

the dynamics of the turbulent velocity fluctuations since it was able to capture the turbulence energy at even the smallest scales even though it was only trained using the classification of the largest scale eddies. The match between the autospectra from the simulated and actual time series, shown in Figure 9, is good. The spatial correlations, shown in Figure 10, are not matched quite as well. Clearly, the integral scales are a bit smaller in the simulation than those from the experiments since only information from adjacent probes was considered to train each network.

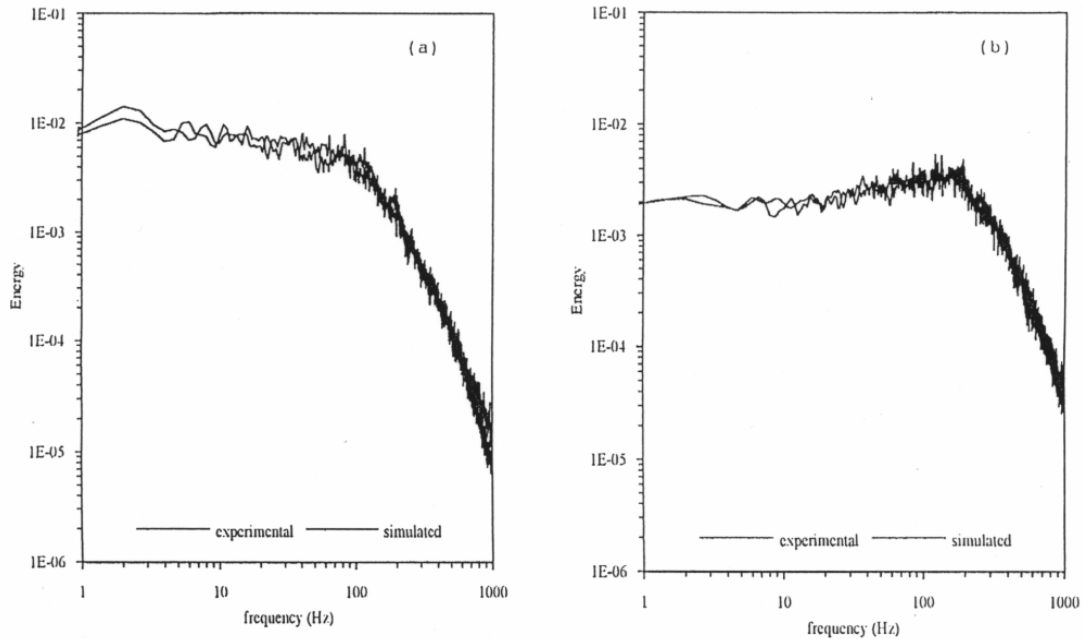


Figure 9: Autospectra of the experimental and simulated (a) streamwise and (b) spanwise velocity components (from [17])

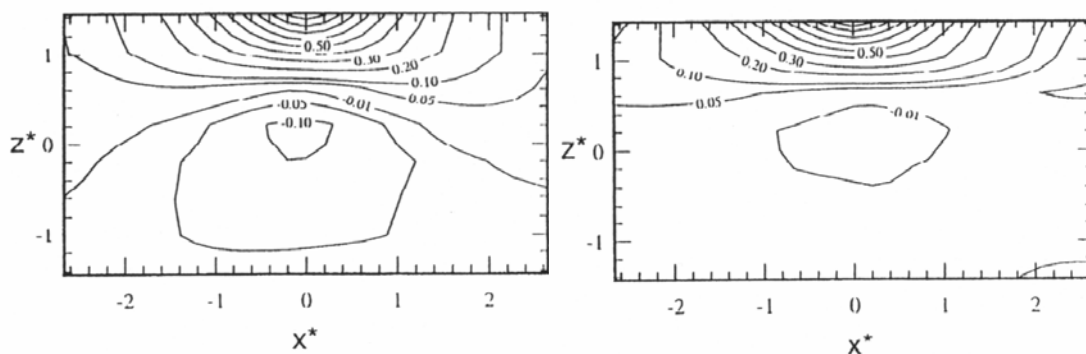


Figure 10: Correlation of the streamwise velocity fluctuations from the (left) experiment and (right) simulation (from [17])

It is interesting to compare the results from this simulation with those for the interpolation with the backpropagation ANN presented in section 3, in particular the autospectra presented

in Figures 6 and 9, acknowledging the completely different flows being examined. The main difference in the results is that the fuzzy ARTMAP is much more able to capture the energy content, in this case, over three orders of magnitude (see Figure 9), compared to less than two for the backpropagation ANN (see Figure 6). We attribute this to the differences in the architecture of the networks; a multilayer perceptron network has a distributed memory while fuzzy ARTMAP is a cognitive classifier with long memory span. The fuzzy clustering aspect of fuzzy ARTMAP possibly allows a wider range of realistic output for a given input pattern because of the independence of the output and input clusters (but which are linked) and the fuzzy membership in those clusters. The backpropagation net is much more deterministic in this regard and we think that adding layers or nodes (the only choice in this form of ANN) cannot overcome this main deficiency (when a higher level of accuracy is desired throughout the spectral range of the data) as it is limited by the stability-plasticity dilemma⁸⁻¹¹. At this point, one should be reminded that the inputs and output of these two examples are similar.

5 SIMULATION OF PRESSURE TIME SERIES

Based on the success in simulating the velocity time series in a turbulent wake, we thought it would be relatively straightforward to simulate the surface pressure fluctuations around a circular cylinder since the range of scales of the energy content of pressure fluctuations is significantly reduced compared to velocities. Galsworthy made his pressure data²⁹ around the surface of a circular cylinder at high Reynolds number ($Re = 10^6$) available to us. At this Reynolds number the flow has a relatively strong vortex shedding as indicated by the spectra of the lift force²⁹. The vortex shedding means two things: the flow field is quasi-periodic and is dominated by large-scale motions, similarly to the fully developed wake considered above. Figure 11 depicts the pressure fluctuations at several locations around the cylinder along with a segment of the lift time series. The lift signal, in particular, shows the vortex shedding frequency (e.g., around 4.2 sec), although there are moments when it appears more erratic (just after 4.3 sec). The pressure time series indicate that the frequency is less pronounced individually except around the separation points (between $90^\circ - 120^\circ$ and $250^\circ - 270^\circ$, where the angle is measured clockwise from the leading edge, 0° ; see Figure 12). Perhaps what is most surprising is that the flow at the trailing edge (180°) exhibits little periodicity, completely different than the flow at lower Reynolds numbers, e.g., $Re = 10^4$. At lower Reynolds numbers, where most wind tunnel experiments are made, the flow is periodic downstream of the separation point and the level of fluctuations is similar. Clearly, this is not the case here as the vortex shedding has been significantly affected by the fact that the boundary layers growing on the surface of the cylinder are turbulent prior to separation. This turbulence apparently mitigates the “communication” between the two separated shear layers so that the periodicity is not transmitted uniformly around the leeward side of the cylinder.

The same modified fuzzy ARTMAP neural architecture as for the velocity simulations (section 4) was used, and the pressure time series were simulated. For this problem, there were 32 networks trained, one for each tap measured. Each net was trained with information from the tap it represented, along with data measured at the same instant in time at its four nearest neighbouring pressure taps. Information at the three previous instants for the main tap

was also used as input, so that there were eight inputs to each network. For example, the ANN for tap 1 (at the leading edge) used the pressure coefficients $C_{p1}(t)$, $C_{p2}(t)$, $C_{p3}(t)$, $C_{p31}(t)$, $C_{p32}(t)$, $C_{p1}(t-1)$, $C_{p1}(t-2)$, and $C_{p1}(t-3)$ for training. In the simulation stage, $C_{p1}(t+1)$ was the output from this net, with the data for $C_{p2}(t)$, etc. coming from the ANN simulations at the other taps so that all data was simulated (except for the initial condition. Note that if we had used entirely experimental data for all prior points, this would be a forecasting problem and the comparison would be with the forecasted and actual measured time series. Since we are running this as a simulation, we can only compare statistics.)

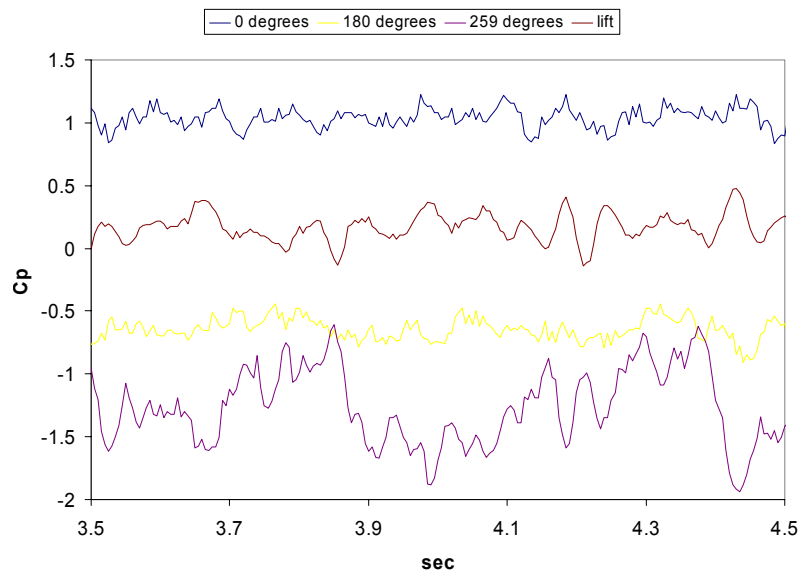


Figure 11: Selected pressure and lift time series around a circular cylinder at $Re=10^6$.

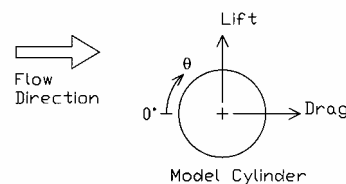


Figure 12. Definition sketch of the flow around the circular cylinder

Selected results are shown in Figure 13. Basically, neural network underestimates the experimentally measured fluctuations and captures incorrect frequency information as well, since it locks onto one of the harmonics. This is most clearly illustrated in the segment of the lift time series. We think that this is due to insufficient temporal information in the training data although there is the possibility that the current data are also insufficient to capture the physics (i.e., the boundary layer turbulence) properly (and we are currently investigating this). The choice of using four adjacent taps and three previous temporal points was based on the spatial and auto-correlations, as was done in the earlier velocity simulation. Takens³⁰ work provides justification for the use of slightly more historical (temporal) points based on the

fractal dimension of the data. However, this limits the patterns being classified to those with lengths less than one period. Therefore, it appears that only the harmonics are being classified since one period of shedding is about 12 points long, not the four used here. Our current work is trying to understand the physical significance of these patterns so that we can use this method with a greater deal of reliability.

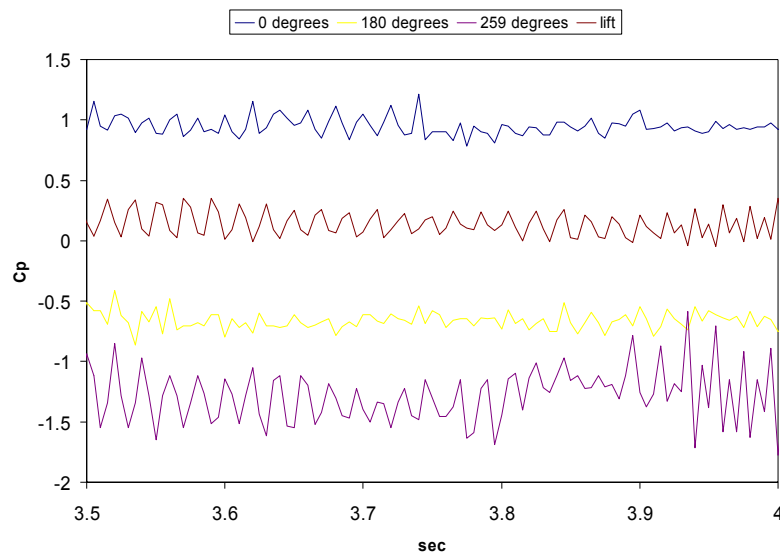


Figure 13: Selected pressure and lift time series around a circular cylinder from the ANN simulation.

6 CONCLUSIONS

Three examples of time series simulations using artificial neural networks were examined. It was shown that performance depended strongly on the type of network, with the fuzzy ARTMAP being superior to the more common backpropagation networks, probably because the former is based on a fuzzy clustering type of pattern recognition, rather than the more deterministic multi-layered backpropagation network. Nevertheless, such a network is useful in applications such as the interpolation problem presented here where a lesser degree of “learning” is required, i.e., no long memory span is required. In addition, the choice of the input and output variables also strongly affects the performance. Basically, the choice of inputs and outputs is determined by the physics of the problem studied, which has to be properly understood if accurate and trustworthy extrapolations are required.

7 ACKNOWLEDGEMENTS

The work presented herein was sponsored by NSERC (Canada) and FM Global Research. Computing support was provided by SHARCNET (Canada). GAK gratefully acknowledges the support of the Canada Research Chairs Program. The authors also wish to acknowledge useful discussions and/or help, with some of the data handling, by Prof. J. Galsworthy, Dr. T.C.E. Ho, Dr. Y. Chen and Dr. P. Senseny. The authors are indebted to Prof. R.A. Antonia

who provided the far wake velocity data.

8 REFERENCES

- [1] K. Gurley, M.A. Tognarelli and A. Kareem, "Analysis and simulation tools for wind engineering", *Prob. Eng. Mech.*, **12**, 9-31 (1997).
- [2] R. Popescu, G. Deodatis and J.H. Prevost, "Simulation of homogeneous nonGaussian stochastic vector fields", *Prob. Eng. Mech.*, **13**, 1-13 (1998).
- [3] M. Gioffrè, V. Gusella and M. Grigoriu, "Simulation of non-Gaussian field applied to wind pressure fluctuations", *Prob. Eng. Mech.*, **15**, 339-345 (2000).
- [4] M. Gioffrè, V. Gusella and M. Grigoriu, "Non-Gaussian wind pressure on prismatic buildings. II. numerical simulation", *ASCE J. Struc. Eng.*, **127**, 990-995 (2001).
- [5] S. Haykin, *Neural networks: a comprehensive foundation*, Macmillian Publishing (1994).
- [6] I. Flood and N. Kartam, "Neural networks in civil engineering I: principles and understanding", *J. Comp. Civ. Eng.*, **8**, 131-148 (1994).
- [7] D.R. Hush and B.G. Horne, "Progress in supervised neural networks: what is new since Lippmann?", *IEEE Signal Proc. Mag.*, 8-39 (Jan.1993).
- [8] G.A. Carpenter and S. Grossberg, "A massively parallel architecture for a self-organizing pattern recognition machine," *Comp. Vision, Graphics Image Proc.*, **37**, 54-115 (1987).
- [9] G.A. Carpenter, S. Grossberg and J.H. Reynolds, "ARTMAP: Supervised real-time learning and classification of nonstationary data by a self-organizing neural network," *Neural Net.*, **4**, 565-588 (1991).
- [10] G.A. Carpenter, S. Grossberg and D. Rosen, "Fuzzy ART: Fast stable learning and categorization of analog patterns by an adaptative resonance system," *Neural Net.*, **4**, 759-771 (1991).
- [11] G.A. Carpenter, S. Grossberg, N. Marcuzon, J.H. Reinolds and D.B. Rosen, "Fuzzy ARTMAP: A Neural Network Architecture for Incremental Supervised Learning of Analog Multidimensional Maps", *IEEE Trans. Neural Net.*, **3**, 698-713 (1992).
- [12] G. Carpenter, S. Grossberg and D. Rosen, "Fuzzy ART: Fast Stable Learning and Categorisation of Analog Patterns by an Adaptive Resonance System", *Neural Net.*, **4**, 759-771 (1991).
- [13] D.E. Rumelhart, G.E. Hinton and R.J. Williams, "Learning internal representations by error propagation", *Parallel Distributed Processing: Explorations in the Microstructure of Cognition* (ed. D.E. Rumelhart and J.L. McClelland), MIT Press, 318-362 (1986).
- [14] J. Ferre-Gine, R. Rallo, A. Arenas and F. Giralt, "Identification of coherent structures in turbulent shear flows with a Fuzzy ARTMAP neural network", *Int. J. Neural Sys.*, **7**, 559-568 (1996).
- [15] J. Ferre-Gine, R. Rallo, A. Arenas and F. Giralt, "Extraction of structures from turbulent signals", *Art. Intel. Eng.*, **11**, 413-419 (1997).
- [16] L. Zadeh, *Fuzzy sets, Information and Control*, **8**, 338-353 (1965).
- [17] F. Giralt, A. Arenas, J. Ferre-Giné, R. Rallo and G.A. Kopp, "The simulation and interpretation of turbulence with a cognitive neural system," *Phys. Fluids*, **12**, 1826-1835 (2000).

- [18] Y. Zhou and R.A. Antonia, "Critical points in a turbulent near wake", *J. Fluid Mech.*, **275**, 59-81 (1994).
- [19] R.J. Adrian and P. Moin, "Stochastic estimation of organized turbulent structure: Homogeneous shear flow," *J. Fluid Mech.*, **190**, 531-559 (1988).
- [20] Y. Chen, G.A. Kopp and D. Surry, "The use of linear stochastic estimation for the reduction of data in the NIST aerodynamic database," *Wind Struct.*, **6**, 107-126 (2003).
- [21] Y. Chen, G.A. Kopp and D. Surry, "Interpolation of wind-induced pressure time series with an artificial neural network," *J. Wind Eng. Ind. Aero.*, **90**, 589-615 (2002).
- [22] H. Ali and P. Senseny, *J. Wind Eng. Ind. Aero.*, to appear (2003).
- [23] H. Tennekes and J.L. Lumley, A first course in turbulence, MIT Press (1972).
- [24] G.A. Kopp, J.G. Kawall and J.F. Keffer, "The evolution of the coherent structures in a uniformly distorted plane turbulent wake," *J. Fluid Mech.*, **291**, 299-322 (1995).
- [25] A. Vernet, G.A. Kopp, J.A. Ferré and F. Giralt, "Three-dimensional structure and momentum transfer in a turbulent cylinder wake," *J. Fluid Mech.*, **394**, 303-337 (1999).
- [26] G.A. Kopp, F. Giralt and J.F. Keffer, "Entrainment vortices and interfacial intermittent turbulent bulges in a plane turbulent wake," *J. Fluid Mech.*, **469**, 49-70 (2002).
- [27] J.A. Ferre and F. Giralt "Pattern recognition analysis of the velocity field in plane turbulent wakes," *J. Fluid Mech.*, **198**, 27-64 (1989).
- [28] A. Vernet and G.A. Kopp, "Classification of turbulent flow patterns with fuzzy clustering," *Eng. App. Art. Intel.*, **15**, 315-326 (2002).
- [29] J. Galsworthy, Aspects of Across-Wind Loads and Effects on Large Reinforced Concrete Chimneys," Ph.D. thesis, University of Western Ontario, 2000.
- [30] F. Takens, "Detecting strange attractors in turbulence," Dynamical systems and turbulence, Lecture Notes in Mathematics, **898**, 366-381 (1981).